# Journal of the American Heart Association

## ORIGINAL RESEARCH

# Extracranial Vascular Anomalies Driven by RAS/MAPK Variants: Spectrum and Genotype–Phenotype Correlations

Vanessa F. Schmidt ![ORCID], MD*; Friedrich G. Kapp ![ORCID], MD*; Constantin Goldann ![ORCID], MD; Linda Huthmann, MD; Beatrix Cucuruz, MD; Richard Brill ![ORCID], MD; Veronika Vielsmeier, MD; Caroline T. Seebauer, MD; Armin-Johannes Michel ![ORCID], MD; Max Seidensticker ![ORCID], MD; Wibke Uller ![ORCID], MD; Jakob B. W. Weiß, MD; Alena Sint, MD; Beate Häberle, MD; Julia Haehl ![ORCID], MD; Alexandra Wagner ![ORCID], MD; Johanna Cordes, MD; Annegret Holm ![ORCID], MD; Denny Schanze ![ORCID], PhD; Jens Ricke, MD; Melanie A. Kimm ![ORCID], PhD; Walter A. Wohlgemuth, MD, PhD; Martin Zenker, MD*; Moritz Wildgruber ![ORCID], MD, PhD*; for the APOLLON Investigators[†]

**BACKGROUND:** We aimed to correlate alterations in the rat sarcoma virus (RAS)/mitogen-activated protein kinase pathway in vascular anomalies to the clinical phenotype for improved patient and treatment stratification.

**METHODS AND RESULTS:** This retrospective multicenter cohort study included 29 patients with extracranial vascular anomalies containing mosaic pathogenic variants (PVs) in genes of the RAS/mitogen-activated protein kinase pathway. Tissue samples were collected during invasive treatment or clinically indicated biopsies. PVs were detected by the targeted sequencing of panels of genes known to be associated with vascular anomalies, performed using DNA from affected tissue. Subgroup analyses were performed according to the affected genes with regard to phenotypic characteristics in a descriptive manner. Twenty-five vascular malformations, 3 vascular tumors, and 1 patient with both a vascular malformation and vascular tumor presented the following distribution of PVs in genes: Kirsten rat sarcoma viral oncogene (n=10), neuroblastoma ras viral oncogene homolog (n=1), Harvey rat sarcoma viral oncogene homolog (n=5), V-Raf murine sarcoma viral oncogene homolog B (n=8), and mitogen-activated protein kinase kinase 1 (n=5). Patients with *RAS* PVs had advanced disease stages according to the Schobinger classification (stage 3–4: *RAS*, 9/13 versus non-*RAS*, 3/11) and more frequent progression after treatment (*RAS*, 10/13 versus non-*RAS*, 2/11). Lesions with Kirsten rat sarcoma viral oncogene PVs infiltrated more tissue layers compared with the other PVs including other *RAS* PVs (multiple tissue layers: Kirsten rat sarcoma viral oncogene, 8/10 versus other PVs, 6/19).

**CONCLUSIONS:** This comparison of patients with various PVs in genes of the RAS/MAPK pathway provides potential associations with certain morphological and clinical phenotypes. *RAS* variants were associated with more aggressive phenotypes, generating preliminary data and hypothesis for future larger studies.

**Key Words:** clinical characteristics ■ mosaicism ■ pathogenic variants ■ RAS/MAPK pathway ■ vascular anomalies

## CLINICAL PERSPECTIVE

### What Is New?

- This study reveals preliminary associations of rat sarcoma virus/V-Raf murine sarcoma viral oncogene homolog B/mitogen-activated protein kinase kinase 1 mosaicism with clinical phenotypes of extracranial vascular anomalies.
- Lesions with Kirsten rat sarcoma viral oncogene pathogenic variants showed more aggressive infiltrative growth patterns across multiple tissue layers, whereas *RAS* variants were characterized by more advanced disease stages and more aggressive phenotypes.

### What Are the Clinical Implications?

- The potential benefit of combining clinical and genetic diagnostics may promote more individualized treatment regimens according to the underlying pathogenic variant, such as adding targeted therapeutics to multidisciplinary care.

### Nonstandard Abbreviations and Acronyms

| | |
|---|---|
| **BRAF** | V-Raf murine sarcoma viral oncogene homolog B |
| **CM** | capillary malformation |
| **HRAS** | Harvey rat sarcoma viral oncogene homolog |
| **KRAS** | Kirsten rat sarcoma viral oncogene |
| **MAPK** | mitogen-activated protein kinase |
| **MAP2K1** | mitogen-activated protein kinase kinase 1 |
| **NRAS** | neuroblastoma ras viral oncogene homolog |
| **PI3K** | phosphatidylinositol 3-kinase |
| **PV** | pathogenic variant |
| **RAS** | rat sarcoma virus |
| **VM** | venous malformation |

Vascular anomalies comprise 2 large entities: vascular tumors and vascular malformations. They are currently categorized mainly on the basis of biological, histopathological, hemodynamic, and clinical findings, as provided by the International Society for the Study of Vascular Anomalies.[1] While vascular malformations are already present at birth and do not regress spontaneously, vascular tumors develop at different ages after birth and may regress on their own. Sporadic vascular malformations are congenital anomalies that are further classified into slow flow malformations (predominantly venous and lymphatic) as well as high-flow arteriovenous malformations (AVMs). While isolated, nonsyndromic slow-flow malformations in most cases follow a benign clinical course, AVMs are characterized by high morbidity, high progression rates, and thus challenging treatment,[2–4] as complete therapy is frequently not possible and the residual lesions continue to progress. The International Society for the Study of Vascular Anomalies classification was last updated in 2018 predominantly on the basis of novel descriptions of genes involved in the development of these rare lesions. More recently, rapidly increasing knowledge about the genetic and molecular basis of vascular malformations has transformed the understanding of the disease mechanisms, potentially allowing improved patient stratification with individualized treatment options.[5] It has been found that sporadic vascular malformations are often caused by somatic gain-of-function variants in genes encoding components of key cellular signaling pathways that regulate growth and differentiation.[6] The wide variability in the clinical phenotype is thought to depend on the cell type affected, the timing of the mutational event, and the degree and nature of pathway activation. In conditions caused by mutations affecting the phosphatidylinositol 3-kinase/protein kinase B/mammalian target of rapamycin signaling pathway, genotype-based stratification has led to early clinical trials of targeted therapies.[7] Somatic activating variants affecting the rat sarcoma virus (RAS)/mitogen-activated protein kinase (MAPK) pathway were first described in intra- and extracranial,[8–10] and preliminary phenotypic correlations were reported.[11–13] The activation of certain signaling pathways not only occurs in vascular endothelial cells but similarly in adjacent soft tissue involving fibroblasts with altered extracellular matrix formation and increased extravascular inflammation.[14] While vascular malformations were formerly regarded as mere dysplastic diseases, the increasing evidence of activated signaling pathways, controlling growth and proliferation, suggests that vascular malformations instead are able to proliferate, which may in part explain the high progression rate reported after incomplete treatment. Therefore, it is currently under debate that malformations instead should be viewed as inborn malformative tumors, and that the dichotomous classification of vascular anomalies into tumors, on the one hand, and vascular malformations, on the other hand, is not accurate anymore.[15] Within this framework, more information is needed comparing the genotype of vascular anomalies with their associated phenotype. We present a cohort of vascular anomalies with mosaic pathogenic variants (PVs) in the V-Raf murine sarcoma viral oncogene homolog B (*BRAF*), mitogen-activated protein kinase kinase 1 (*MAP2K1*), and *RAS* genes detected by ultra-deep next-generation sequencing

of affected tissue. Phenotypic and clinical associations including treatment response and recurrence are reported.

## METHODS

The data sets used and analyzed during the current study are available from the corresponding author on reasonable request.

### Primary Aim of the Study

This study aimed to correlate certain clinical phenotypes to genetic alterations in the RAS/MAPK pathway in a descriptive manner. Clinical features,[16–18] lesion extension, and progression rates are included as part of the phenotype.

### Patient Cohort and Sample Collection

This retrospective multicenter cohort study was conducted by multidisciplinary vascular anomaly centers of 5 university hospitals in Germany, seeing a minimum of 150 new patients with vascular anomalies annually. Retrospective analyses were approved by the local ethics committee (University Hospital, LMU Munich), Project No. 23-0337 (06/29/2023). All patients signed informed consent to participate. The Strengthening the Reporting of Genetic Association Studies[19] guidelines were used for appropriate reporting.

Core needle biopsies were collected between January 2019 to March 2023 under ultrasound guidance close to the center/nidus of the vascular lesion during invasive treatment or clinically indicated biopsies (before planned targeted therapy). Patients not receiving therapy do not routinely undergo biopsies for genetic testing at the participating institutions. Patients were eligible for this study, if a pathogenic variant in the RAS (Kirsten rat sarcoma viral oncogene [KRAS], Harvey rat sarcoma viral oncogene homolog [HRAS], neuroblastoma ras viral oncogene homolog [NRAS]), V-Raf murine sarcoma viral oncogene homolog B (BRAF), or MAP2K1 genes was proven in fresh or formalin-fixed paraffin-embedded tissue biopsies from the vascular lesion. Exclusion criteria were clinical, pathological, or radiological doubts regarding the diagnosis of a vascular anomaly. Demographics, medical history, and clinical and radiological data, as well as treatment course and follow-up assessments, were collected. Disease recurrence, when suspected clinically, was evaluated by magnetic resonance imaging. Increase or reoccurrence of clinical symptoms after treatment as well as increased lesion size or newly perfused vessels on magnetic resonance imaging compared with imaging findings after the last treatment was defined as progression.

### DNA Extraction

Genomic DNA was extracted from native tissue samples and deparaffinated formalin-fixed paraffin-embedded samples using the QIAamp DNA Mini Kit (Qiagen, Hilden, Germany) following the manufacturer's instructions. DNA concentration was measured using a Qubit 4 fluorometer (Invitrogen, Carlsbad, CA) and adjusted according to the requirements of subsequent experiments.

### Mosaic Variant Screening

Methods for mosaic variant detection evolved during the course of this project. Initially, Sanger sequencing of KRAS, HRAS, NRAS, BRAF, and MAP2K1 hotspot exons was used, reaching a mosaic detection threshold of 10% to 15% variant allele frequency. To this end, mutation hotspot exons with flanking introns were amplified by polymerase chain reaction (PCR), and bidirectional Sanger sequencing was performed using a Big Dye Terminator Cycle Sequencing Kit on a 3500xl Genetic Analyzer (Applied Biosystems, Foster City, CA). Sequences were aligned using the Seqpilot analysis software (JSI Medical Systems, Kippenheim, Germany). Mosaic level for mutations was estimated by comparing the area under the curve of electropherograms for the wild type and mutant peaks in the forward and reverse sequencing directions.

The majority of samples were investigated by ultradeep sequencing of targeted multigene panels. This was carried out by paired-end sequencing with 2×151 bp reads on a MiSeq system or NextSeq 550 system (Illumina, San Diego, CA) to obtain for each sample an average of 2.5M or 20M reads, respectively. Different target enrichment kits either with or without molecular barcoding by unique molecular identifiers were used during the course of this project: Illumina TruSeq Custom Amplicon Panel; Agilent SureSelect XT HS2 DNA Custom Panel with unique molecular identifiers (random 3-bp duplex) (Agilent Technologies, Santa Clara, CA); Twist EF Custom Library Prep 2.0 of a Twist Custom Panel with Twist UMI Adapter (fixed 5-bp or 6-bp duplex) (Twist Bioscience, South San Francisco, CA). The target sequence comprised a panel of genes/gene hotspots that are known to be involved in vascular malformations or regional overgrowth. The gene content evolved over time (a complete list of genes/gene hotspots covered by the employed enrichment kit is available in Table S1). Library preparation was performed according to the respective manufacturer's instructions. Indexed sample libraries were equimolarly pooled for final multiplexed sequencing. Samples that underwent initial screening by Sanger sequencing and remained negative were not systematically reassessed by next-generation sequencing later. Therefore, we may have missed cases with RAS/MAPK pathway

mosaic variants, because variant allele frequencies for causative variants in mixed-tissue DNA samples from vascular malformations are often <15%. However, as only mutation-positive cases are reported and analyzed in this article, the results and conclusions are unlikely to be affected by false-negative cases in the baseline cohort.

## Genomic Data Analyses

Raw data (bcl format, binary base call sequence files) were uploaded to the varvis software package (Limbus Medical Technologies GmbH, Rostock, Germany) and processed (demultiplexing, read alignment, error correction) using the GRCh37 reference genome and the bioinformatics pipeline from varvis software version 1.23.3 with the manufacturer's standard settings. For unique molecular identifiers analysis (duplex sequencing data processing), duplex barcode sequences were extracted from the read sequence according to the manufacturer's user manual (Agilent SureSelect XT HS2 DNA Kits Protocol or Twist EF Library Preparation Kit, respectively) and reads were aligned to the reference genome. A minimum of 2 reads were required to define a strand-specific consensus read. Strand-specific consensus reads were then combined to create a final consensus read. Variant consensus reads were called down to a minimum variant allele frequency of 0.5% with a minimum of 2 aberrant consensus reads, thereby reaching a detection threshold for mosaic variants of at least 0.5% for most samples. The target regions typically had a mean sequencing depth of >2000× after demultiplexing, except for DNA samples from formalin-fixed paraffin-embedded tissue, which yielded variable but usually lower coverage.

## Variant Confirmation By Digital PCR

Variants with an allele frequency close to the detection threshold were verified by digital PCR. Digital PCR was performed on a QIAcuity Four Digital PCR System (Qiagen, Hilden, Germany) on 26 k nanoplates using the QIAcuity Probe PCR Kit and digital PCR LNA Mutation Assays (QIAGEN GmbH, Hilden, Germany) containing specific probes for wild type as well as mutant alleles. Data analysis was performed using the QIAcuity Software Suite 2.1.8.23. The detection limit for the target variants was 0.1%.

## Statistical Analysis

To analyze age and follow-up time, the data were presented as median (range, minimum–maximum). Subgroup analyses were performed related to the affected genes. We used Fisher's exact test for categorial data and small sample sizes to assess the association of the different PV carriers with clinical phenotypes defined as lesion localization, lesion tissue involvement, Cho classification,[16] Schobinger classification,[17] extremity length discrepancy (yes/no), and associated segmental overgrowth (yes/no), as well as with therapy response defined as progression (yes/no). Analysis was conducted using SPSS version 26.0 (IBM Corp., Armonk, NY); all *P* values reported were 2-tailed.

# RESULTS

## Patient Characteristics and Clinical Presentation

All patients included presented with clinically and radiologically confirmed extracranial vascular anomalies, had a somatic mutation in genes of the RAS pathway, and received multimodal treatment according to the anomaly type, clinical presentation, and patient preference (embolization, sclerotherapy, surgery, targeted medical therapy). Twenty-nine patients were included in the study (Table 1) with a median age of 20 years (range, 5–55 years) at the time of genetic testing. The cohort consisted of 18 of 29 (62.1%) women and 11/29 (37.9%) men. All patients had extracranial vascular anomalies, 25 of 29 (86.2%) patients had vascular malformations, and 3 of 29 (10.3%) patients had benign vascular tumors, according to the International Society for the Study of Vascular Anomalies classification.[20] One patient (1/29, 3.4%) presented with both a vascular malformation (capillary malformation [CM]) as well as an additional vascular tumor (pyogenic granuloma), which was located on the CM. The mean age of the patients at clinical manifestation of the lesions was 2 years (range, 0–39 years). Vascular anomalies were located on the lower extremities in 11 of 29 patients (37.9%), followed by the head and neck region (5/29, 17.2%), the upper extremities (4/29, 13.8%), and the trunk (4/29; 13.8%). Five extensive lesions (5/29, 17.2%) involved the trunk as well as upper or lower extremities. Among all cases with vascular malformations, 24 of 26 (92.3%) patients presented simple or combined AVMs, while there was 1 of 26 (3.8%) simple venous malformation (VM) as well as 1 of 26 (3.8%) CM (Table 1). The distribution of AVMs according to the clinical Schobinger classification (n=24) was as follows: stage 1 (2/24, 8.3%), stage 2 (10/24, 41.7%), stage 3 (10/24, 41.7%), and stage 4 (2/24, 8.3%). AVMs were further classified angiographically according to the Cho classification (n=24): type I (1/24, 4.2%), type II (1/24, 4.2%), type IIIa (12/24, 50.0%), and type IIIb (10/24, 41.7%).

## Treatment Course and Follow-Up

In 23 of 29 (79.3%) cases, the vascular anomalies were treated by minimally invasive procedures (AVM

**Table 1. Patient Characteristics and Clinical Presentation of Study Cohort**

| Patient no. | Age, y | Sex | Type of vascular anomaly | Subtype of vascular lesion | Tissue involvement | Lesion localization | Segmental overgrowth | Extremity length discrepancy | CNS occupancy | Angiographic classification (Cho*/Puig†) | Schobinger classification‡ | Treatment | Progression |
|---|---|---|---|---|---|---|---|---|---|---|---|---|---|
| 1 | 5 | m | Vascular malformation | Combined (CVAVM) | (Sub)cutaneous | LE | Ipsilateral | | | IIIa* | 2 | Embolization | Yes |
| 2 | 34 | m | Vascular malformation | Arteriovenous | Multiple layers | LE | Ipsilateral | Yes | | IIIa* | 3 | Embolization+resection | Yes |
| 3 | 22 | w | Vascular malformation | Arteriovenous | Multiple layers | UE | | | | IIIb* | 3 | Embolization | Yes |
| 4 | 54 | m | Vascular malformation | Arteriovenous | Multiple layers | LE | Ipsilateral | Yes | | II* | 3 | Embolization+resection | Yes |
| 5 | 17 | w | Vascular tumor | Benign | Multiple layers | Trunk+LE | | | | … | … | Embolization | No |
| 6 | 26 | w | Vascular malformation | Arteriovenous | Multiple layers | HN | | | | IIIb* | 3 | Embolization+targeted therapy (VEGF inhibitor+MEK inhibitor) | No |
| 7 | 17 | w | Vascular malformation | Syndromic (Parkes–Weber-like phenotype) | Multiple layers | LE | Ipsilateral | Yes | | IIIa* | 3 | Sclerotherapy+embolization | Yes |
| 8 | 21 | w | Vascular malformation | Arteriovenous (IFFVA) | Intramuscular | UE | Ipsilateral | | | IIIa* | 2 | None | NA |
| 9 | 55 | m | Vascular malformation | Arteriovenous | Multiple layers | Trunk+UE | Ipsilateral | | | IIIb* | 3 | Embolization+resection | Yes |
| 10 | 34 | w | Vascular malformation | Arteriovenous | Multiple layers | LE | Ipsilateral | | | IIIb* | 4 | Embolization | NA |
| 11 | 14 | w | Vascular malformation | Combined (CAVM) | Multiple layers | LE | Ipsilateral | Yes | | IIIa* | 3 | Embolization | Yes |
| 12 | 17 | m | Vascular malformation | Combined (CVAVM) | Multiple layers | LE | Ipsilateral | | | I* | 2 | Embolization | Yes |
| 13 | 20 | w | Vascular malformation | Arteriovenous | Intramuscular | UE | | | Yes | IIIb* | 3 | Embolization | Yes |
| 14 | 25 | m | Vascular tumor | Benign | Intramuscular | Trunk | Ipsilateral | | | … | … | Embolization+resection | Yes |
| 15 | 20 | m | Vascular malformation | Arteriovenous (IFFVA) | Intramuscular | Trunk | Ipsilateral | | | IIIb* | 2 | Resection | No |
| 16 | 14 | w | Vascular malformation (1)+vascular tumor (2) | CM (1) +benign (Pyogenic granuloma within CM; 2) | (Sub)cutaneous | Trunk | | | | … | … | None | NA |
| 17 | 2 | w | Vascular malformation | Arteriovenous | Intramuscular | HN | | | | IIIa* | 2 | Embolization | No |

*(Continued)*

**Table 1.  Continued**

| Patient no. | Age, y | Sex | Type of vascular anomaly | Subtype of vascular lesion | Tissue involvement | Lesion localization | Segmental overgrowth | Extremity length discrepancy | CNS occupancy | Angiographic classification (Cho*/Puig†) | Schobinger classification‡ | Treatment | Progression |
|---|---|---|---|---|---|---|---|---|---|---|---|---|---|
| 18 | 17 | w | Vascular malformation | Arteriovenous | Intramuscular | LE | | | | IIIa* | 3 | Embolization+resection | No |
| 19 | 4 | w | Vascular tumor | Benign | (Sub)cutaneous | Trunk | | | | … | … | Embolization+resection | No |
| 20 | 10 | w | Vascular malformation | Arteriovenous | Multiple layers | LE | | | | IIIa* | 3 | Targeted therapy (BRAF inhibitor) | No |
| 21 | 2 | m | Vascular malformation | Syndromic (Parkes–Weber-like phenotype) | Multiple layers | Trunk+LE | Ipsilateral | Yes | | IIIb* | 1 | None | NA |
| 22 | 33 | w | Vascular malformation | Arteriovenous | Intramuscular | LE | Ipsilateral | Yes | | IIIa* | 2 | Embolization | NA |
| 23 | 50 | w | Vascular malformation | Arteriovenous | (Sub)cutaneous | Trunk+LE | | | | IIIb* | 1 | Embolization | No |
| 24 | 35 | w | Vascular malformation | Venous | (Sub)cutaneous | UE | | | | 1† | … | Resection | Yes |
| 25 | 25 | m | Vascular malformation | Arteriovenous | Multiple layers | LE | | | | IIIb* | 2 | Embolization | No |
| 26 | 25 | w | Vascular malformation | Arteriovenous | Multiple layers | Trunk+UE | Ipsilateral | Yes | | IIIa* | 4 | Embolization+targeted therapy (MEK inhibitor) | No |
| 27 | 20 | m | Vascular malformation | Arteriovenous | (Sub)cutaneous | HN | Ipsilateral | | | IIIb* | 2 | Embolization+resection | No |
| 28 | 21 | m | Vascular malformation | Arteriovenous | (Sub)cutaneous | HN | | | | IIIa* | 2 | Embolization+resection | Yes |
| 29 | 16 | w | Vascular malformation | Arteriovenous | (Sub)cutaneous | HN | | | | IIIa* | 2 | Embolization+resection | No |

CAVM indicates capillary arteriovenous malformation; CM, capillary malformation; CNS, central nervous system; CVAVM, capillary venous arteriovenous malformation; HN, head and neck; IFFVA, intramuscular fast-flow vascular anomaly; LE, lower extremity; m, man; MEK, mitogen-activated protein kinase kinase enzymes; NA, not available; UE, upper extremity; VEGF, vascular endothelial growth factor; and w, woman.

*Cho classification according to Cho et al.[16]

†Puig classification according to Puig et al.[18]

‡Schobinger classification according to Finn et al.[17]

embolization, VM sclerotherapy), in 11 of 29 (37.9%) cases a surgical resection was performed, and in 3 of 29 (10.3%) cases, patients received targeted medical therapies. The median follow-up time was 23 months (range, 8–37 months). Overall, 12 of 24 (50.0%) patients experienced a progression in the clinical course after treatment. The individual treatment modalities and progression rates, as part of the phenotypic characterization, are described in detail in Table 1.

## Mutational Spectrum in Extracranial Vascular Anomalies

The identified PVs involved *RAS* genes in 16 of 29 (55.2%) cases (see Figure 1): *KRAS* (10/29, 34.5%), *HRAS* (5/29, 17.2%), and *NRAS* (1/29, 3.4%). We also found PVs in *BRAF* (8/29, 27.6%; see Figure 2) and *MAP2K1* (5/29, 17.2%; see Figure 3). Variant allele frequencies in DNA from lesional tissue samples ranged from 1% to 30% (Table 2). We identified 17 distinct PVs:

5 in *KRAS*, 5 in *HRAS*, 1 in *NRAS*, 2 in *BRAF*, and 4 in *MAP2K1*. Four PVs (c.1799T>A, p.Val600Glu in *BRAF*; c.35G>A, p.Gly12Asp in *KRAS*; c.183A>C, p.Gln61His in *KRAS*; c.171G>T, and p.Lys57Asn in *MAP2K1*) were recurrently observed in our cohort in 7/29 (24.1%), 5 of 29 (17.2), 2 of 29 (6.9%), and 2 of 29 (6.9%) patients, respectively. All other PVs were only identified once. None of the identified PVs was detected in leukocyte DNA or in control tissue samples, when available.

## Genotype–Phenotype Associations

A comparison of clinical characteristics between patients with *RAS*, *BRAF*, and *MAP2K1* PVs is shown in Table 3. Patients with *RAS* PVs had a higher score according to Schobinger classification (3.0 [range, 2–4] versus 2.0 [range, 1–3] versus 2.0 [range, 2–4]; $P=0.037$) and progression after treatment was more frequently observed (76.9% versus 16.7% versus 20.0%; $P=0.024$). There were no remarkable differences in the
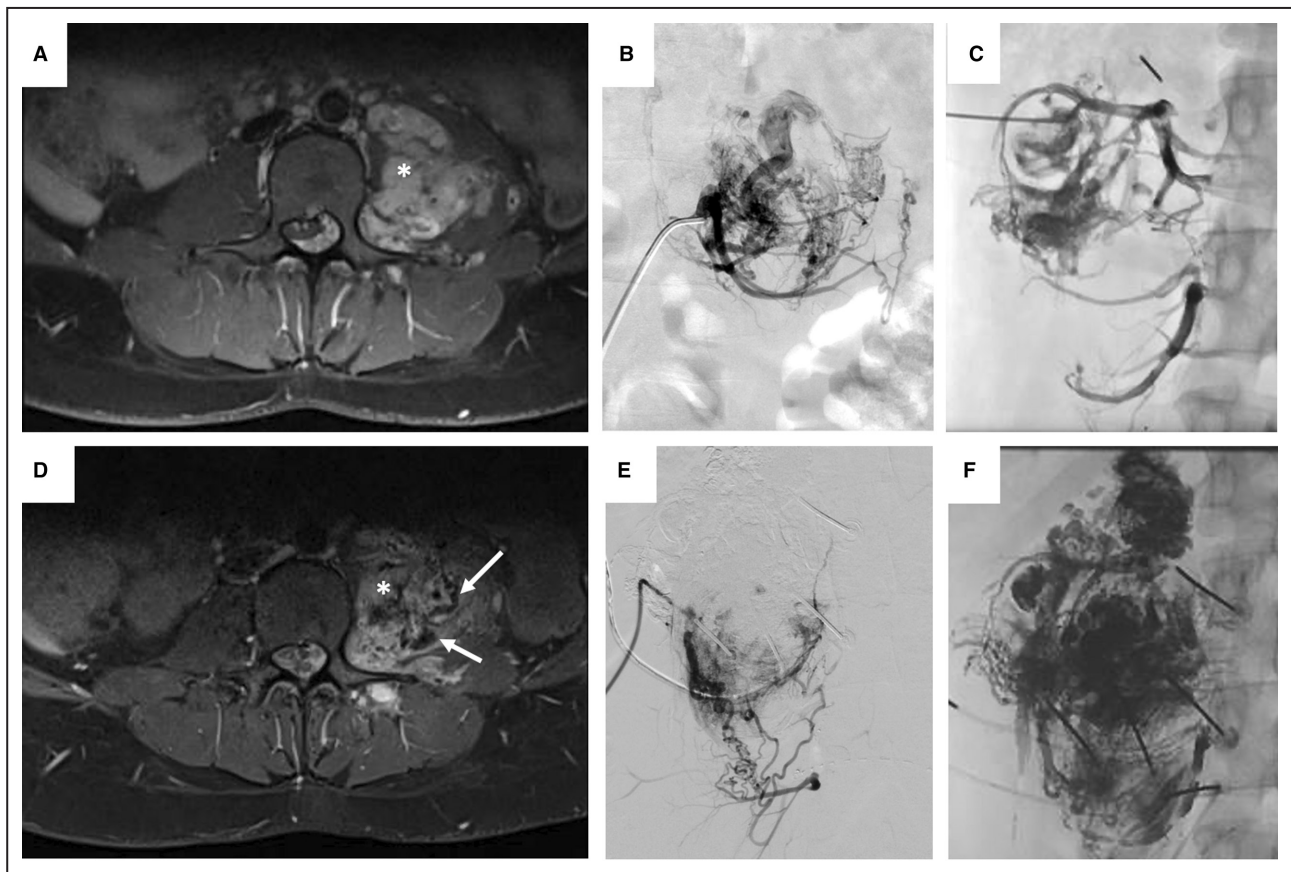


**Figure 1.  Patient 1: 20-year-old female patient with arteriovenous malformation (AVM) paravertebral and a *HRAS* pathogenic variant (PV).**
**A**, Axial T1-weighted turbo spin-echo sequence image presenting an AVM (asterisk) located paravertebrally on the left side with intramuscular extension and involvement of the spinal canal and compression of the dural tube. Digital subtraction image before (**B**) and after (**C**) the first session of embolotherapy with ethylene-vinyl-alcohol copolymer (Squid-18, BALT Germany GmbH). **C**, The image shows near complete embolization of the lesion (2020). **D**, Axial T1-weighted turbo spin-echo sequence image after 3 sessions of embolization presenting newly perfused vessels confirming clinically suspected progression, which was characterized by increasing pain and functional movement impairment (2023). Preprocedural (**E**) and periprocedural (**F**) digital subtraction images of the fourth embolotherapy session, both showing the newly embolized vascularized components of the progressive AVM (2023).
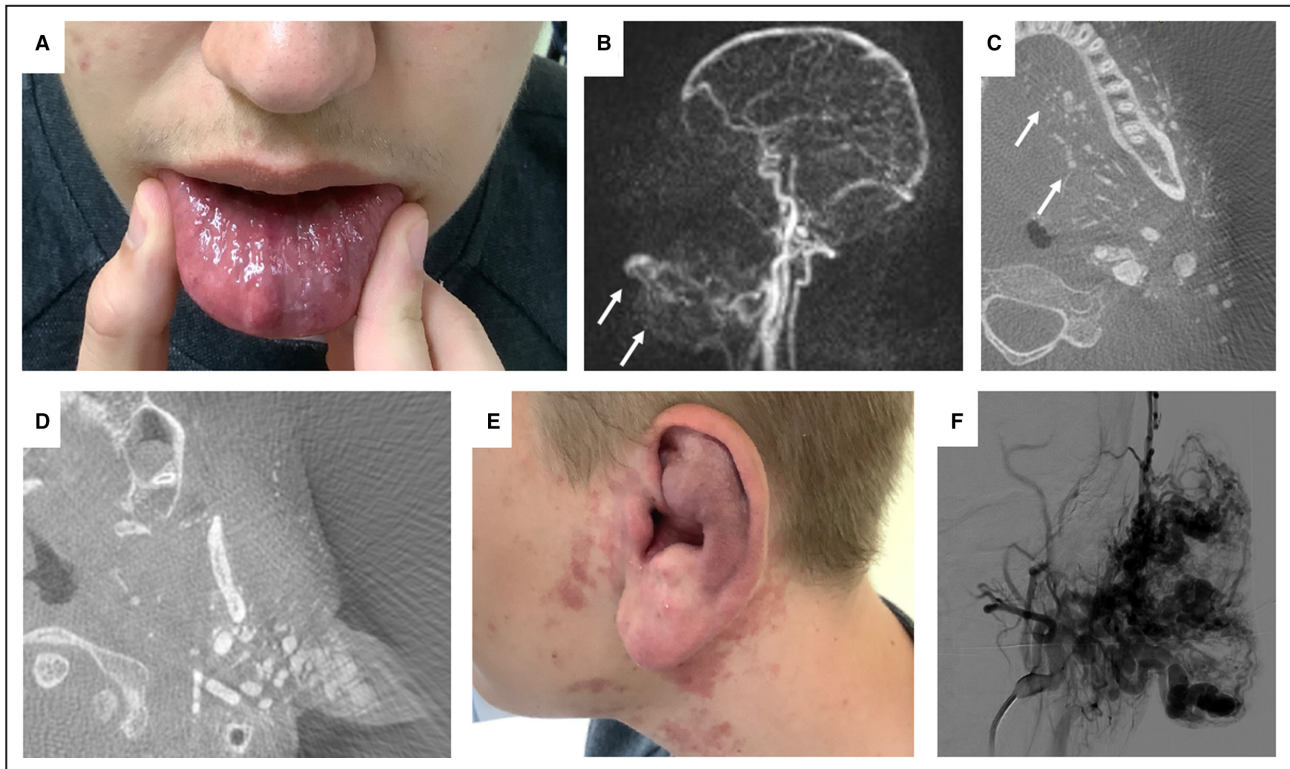
**Figure 2.  Patient 27: 20-year-old male patient with an infiltrative phenotype and a *MAP2K1* pathogenic variant (PV).**
**A**, Clinical infiltration of the lip; notice the prominent blood vessels on the left side of the lower lip. **B**, Time-resolved angiography with interleaved stochastic trajectories showing contrast enhancement of the lip and around the mandible. **C** and **D**, Contrast-enhanced vessels in computed tomography reconstruction of the digital subtraction angiography. Notice the fine vessels infiltrating the tongue and the left side of the face, most prominent at the base of the ear. **E**, Correlating to the prominent vessels at the base of the ear is the enlarged ear, including the ear lobe. **F**, Digital subtraction angiography of the ear, demonstrating 3 large feeders into the outer ear.

prevalence of clinical manifestations such as leg length discrepancy, associated segmental overgrowth or in the angiographic classification according to Cho (see Table 3). In addition, there was no evident association between lesion localization and the different genotypes (see Table 3).

Lesions with *KRAS* PVs infiltrated multiple tissue layers more frequently than subcutaneous or muscular tissue only compared with the other PVs (*KRAS*, 80.0% versus *HRAS*, 40.0% versus *NRAS*, 0.0% versus *BRAF*, 25.0% versus *MAP2K1*, 40.0%; $P=0.036$; see Table 4).

## DISCUSSION

This retrospective multicenter cohort study describes potential correlations between mosaic-activating PVs in 5 genes of the RAS/MAPK pathway (*KRAS*, *HRAS*, *NRAS*, *BRAF*, and *MAP2K1*) and phenotypic characteristics. Lesions with *KRAS* PVs showed a more aggressive infiltrative growth pattern across multiple tissue layers. Furthermore, *RAS* variants were characterized by more advanced disease stages and higher progression rates. No differences were observed in the angiographic classification of lesions or in the prevalence of

associated disease manifestations such as leg length discrepancy and segmental overgrowth.

Initially, *KRAS* PVs in vascular anomalies were mainly described in intracranial vascular malformations[9,21,22] but more recent studies have increasingly reported them in extracranial lesions.[8,11,23] Al-Olabi et al[8] found *KRAS* PVs in 4 of 135 patients with slow-flow malformations and in 3 of 25 patients with extracranial AVMs. In intracranial AVMs, *KRAS* PVs are mostly found at the hotspot in codon 12 (G12V and G12D), which is also frequently mutated in cancer. In accordance with this, 50% of *KRAS* PVs in our study were c.35G>A, p.Gly12Asp (G12D). In 2 cases, we found the *KRAS* PV c.183A>T, p.Gln61His (Q61H). This PV was reported by El Sissy et al[11] as the most frequent distinct variant (67%) in their cohort consisting of 6 extracranial AVMs with *KRAS* PVs. Various other *KRAS* PVs have been reported in vascular anomalies. Ten Broek et al[13] presented 8 different variants in a cohort with 9 *KRAS* PVs, which were found in various types of vascular malformations. In addition to the most prevalent *KRAS* variants, we identified 5 *HRAS* PVs and 1 *NRAS* PV that were nonrecurrent in our cohort. Notably, all observed *HRAS* PVs represented in-frame deletions/
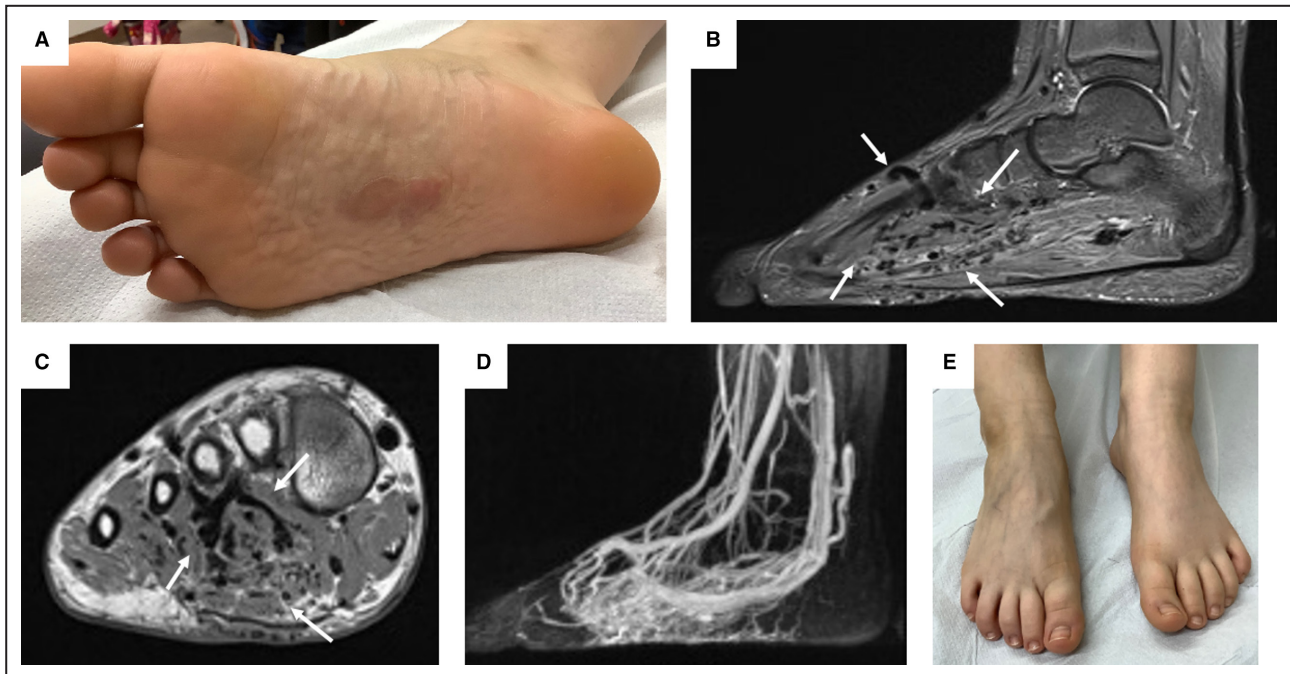
**Figure 3.  Patient 20: 10-year-old female patient with an infiltrative arteriovenous malformation and a *BRAF* pathogenic variant (PV).**

**A**, Clinical manifestation with capillary malformation (CM) of the sole of the right foot; also note the wormlike mass and dilated veins. **B** and **C**, Sagittal T2-weighted turbo-inversion recovery-magnitude and coronal T1-weighted turbo spin-echo sequence images; note the flow voids in deeper tissues of the foot (labeled with white arrows). **D**, Time-resolved angiography with interleaved stochastic trajectories angiography showing the marked hyperperfusion of the foot including cutaneous tissue. **E**, Correlating to the hyperperfusion, dilated veins can be seen on the back of the affected right foot of the patient.

insertions affecting the switch-II region (amino acids 58–76) of the HRAS protein. Eijkelenboom et al[24] presented five *HRAS* in frame insertions in that region in patients with vascular malformations/overgrowth syndromes and provided functional data that showed the inability of guanine nucleotide exchange factors to induce GTP loading and reduced intrinsic and GTPase-activating protein–stimulated GTP hydrolysis of mutant HRAS proteins. These opposing effects led to a net increase in MAPK activation in a cellular model system and were supposed to cause decoupling from activating upstream cellular signals. Our observations provide further evidence that variants of that particular type are characteristic of *HRAS* PVs associated with vascular anomalies, which often present as atypical vascular malformation/overgrowth syndromes. The *HRAS* PV c.172_177delinsGTCCTGGATGTT, p.Thr58_Ala59delinsValLeuAspVal, which was found in 1 of our patients, has previously been reported by Konczyk et al[25] in a patient with facial AVM and associated adipose tissue overgrowth of the right cheek. Our patient with this distinct variant presented with an extensive AVM of the lower extremity, associated capillary lesions, leg length discrepancy, and segmental overgrowth, as well as recurrent pain (patient 11). There was no difference observed between the patients with

*HRAS* versus *KRAS* PVs in our cohort regarding the occurrence of clinical characteristics, such as segmental overgrowth. Consistent with our findings, *NRAS* PVs tend to be in the minority in most cohorts reporting vascular anomalies and *RAS* variants.[8,26] In the literature, 1 distinct *NRAS* PV, c.182A>G, p.Gln61Arg (Q61R), was recurrently identified in complex lymphatic anomalies, such as generalized lymphatic anomaly or kaposiform lymphangiomatosis.[27–30] However, the *NRAS* PV affecting the same codon, c.183A>T, p.Gln61His, was confirmed in 1 patient presenting with a CM on the costal arch and a vascular tumor (pyogenic granuloma) located on this CM. Consistent with this, Ten Broek et al[13] described 1 case with both multiple eruptive pyogenic granulomas and a CM with the same *NRAS* PV. In addition, a cohort of patients with pyogenic granuloma was reported, in which 1 *NRAS* PV was found, while most of pyogenic granulomas contained *GNAQ* PVs.[31] Interestingly, *NRAS* PVs have not been reported in AVMs so far, either in our series or in the literature. Concerning all 16 cases with *RAS* PVs in our cohort, we noticed that these anomalies presented mainly with complex phenotypes, such as extensive combined vascular malformations or associated segmental overgrowth (68%). Additionally, among these 16 cases, there were 2 intramuscular hemangioma-like

**Table 2.** Mutational Spectrum and Genotypic Characterization of Study Cohort

| Patient no. | Gene | cDNA; amino acid change | Source | Technology | Mutant allele fraction, % | Mutant allele count | Total allele count | dPCR confirmation, % |
|---|---|---|---|---|---|---|---|---|
| 1 | KRAS | c.35G>A; p.(Gly12Asp) | Native tissue (2) | Ultra-deep NGS | 14.2<br>8.6 | 661<br>210 | 4661<br>2456 | 9.4<br>7.5 |
| 2 | KRAS | c.34G>T; p.(Gly12Cys) | Native tissue | Ultra-deep NGS | 8.7 | 47 | 540 | 10.5 |
| 3 | KRAS | c.35G>A; p.(Gly12Asp) | Native tissue | Ultra-deep NGS+UMI | 8.2 | 104 | 1273 | 5.4 |
| 4 | KRAS | c.183A>C; p.(Gln61His) | Native tissue | Ultra-deep NGS+UMI | 6.7 | 135 | 2024 | 5.7 |
| 5 | KRAS | c.182A>G; p.(Gln61Arg) | Native tissue | Ultra-deep NGS | 7.6 | 731 | 9610 | 7.6 |
| 6 | KRAS | c.183A>C; p.(Gln61His) | Native tissue | Ultra-deep NGS+UMI | 9.4 | 106 | 1130 | 7.7 |
| 7 | KRAS | c.35G>A; p.(Gly12Asp) | Native tissue | Sanger NGS | 4.5 | 73 | 1619 | NA |
| 8 | KRAS | c.188_229dup; p.(Glu63_Glu76dup) | Native tissue | Ultra-deep NGS+UMI | 4.7 | 122 | 2500 | NA |
| 9 | KRAS | c.35G>A; p.(Gly12Asp) | FFPE tissue | Ultra-deep NGS+UMI | 4.5 | 76 | 1703 | 4.0 |
| 10 | KRAS | c.35G>A; p.(Gly12Asp) | Native tissue | Ultra-deep NGS+UMI | 8.7 | 148 | 1698 | 11.4 |
| 11 | HRAS | c.172_177delinsGTCCTGGATGTT; p.(Thr58_Ala59delinsValLeuAspVal) | Native tissue | Ultra-deep NGS | 6.7 | 37 | 535 | NA |
| 12 | HRAS | c.191_217dup; p.(Met72_Arg73insHisSerAlaMetArgAspGlnTyrMet) | Native tissue | Ultra-deep NGS+UMI | 15.0 | 322 | 2146 | NA |
| 13 | HRAS | c.172_179delins; p.(Thr58_Gly60delinsValLeuAspValLeu) | FFPE tissue | Ultra-deep NGS+UMI | 6.9 | 162 | 2331 | NA |
| 14 | HRAS | c.215_216insTTCCAGCGCCATGCGGGACCAGTACAT; p.(Tyr71_Met72insIleSerSerAlaMetArgAspGlnTyr) | Native tissue | Ultra-deep NGS+UMI | 7.0 | 113 | 1614 | NA |
| 15 | HRAS | c.217_218ins27; p.(Met72_Arg73insProSerAlaMetArgAspGlnTyrMet) | FFPE tissue | Ultra-deep NGS+UMI | 11.0 | 118 | 1077 | NA |
| 16 | NRAS | c.183A>T; p.(Gln61His) | Native tissue | Ultra-deep NGS | 7.7 | 544 | 7031 | NA |
| 17 | BRAF | c.1517+2_1517+3insTACTCAGGT; p.? | Native tissue | Ultra-deep NGS+UMI | 23.0 | 631 | 2744 | NA |
| 18 | BRAF | c.1799T>A; p.(Val600Glu) | Native tissue | Ultra-deep NGS | 2.8 | 343 | 12296 | 3.7 |
| 19 | BRAF | c.1799T>A; p.(Val600Glu) | FFPE tissue | Ultra-deep NGS | 30.3 | 5118 | 16913 | 37.0 |
| 20 | BRAF | c.1799T>A; p.(Val600Glu) | Native tissue | Sanger | 23 | … | … | 15.3 |
| 21 | BRAF | c.1799T>A; p.(Val600Glu) | Native tissue | Ultra-deep NGS+UMI | 5.7 | 94 | 1656 | 5.3 |
| 22 | BRAF | c.1799T>A; p.(Val600Glu) | Native tissue | Ultra-deep NGS+UMI | 10.4 | 191 | 1828 | 12.8 |
| 23 | BRAF | c.1799T>A; p.(Val600Glu) | Native tissue | Ultra-deep NGS+UMI | 4.0 | 71 | 1754 | 7.2 |
| 24 | BRAF | c.1799T>A; p.(Val600Glu) | Native tissue | Ultra-deep NGS | 9.5 | 218 | 2287 | NA |
| 25 | MAP2K1 | c.171G>T; p.(Lys57Asn) | Native tissue (2) | Sanger | 16<br>18 | …<br> | …<br> | NA |
| 26 | MAP2K1 | c.169_170delinsCC; p.(Lys57Pro) | Native tissue (2) | Sanger | 16<br>20 | …<br> | …<br> | NA |
| 27 | MAP2K1 | c.167A>C; p.(Gln56Pro) | Native tissue | Ultra-deep NGS+UMI | 10.9 | 21 | 192 | NA |
| 28 | MAP2K1 | c.171G>T; p.(Lys57Asn) | Native tissue | Ultra-deep NGS+UMI | 9.7 | 474 | 4886 | NA |
| 29 | MAP2K1 | c.171_185del; MAP2K1; p.(Gln58_Glu62del) | Native tissue | Ultra-deep NGS+UMI | 0.9 | 15 | 1588 | NA |

dPCR indicates digital polymerase chain reaction; FFPE, formalin-fixed paraffine-embedded tissue; FT, fresh tissue; NA, not available; NGS, next-generation sequencing; and UMI, unique molecular identifiers.

**Table 3.   Comparison of Clinical Characteristics Among the RAS, BRAF, and MAP2K1 PV Carriers**

| Clinical characteristics | RAS | BRAF (n) | MAP2K1 | P value[‡] |
|---|---|---|---|---|
| Age, y | n=16 | n=8 | n=5 | |
| Median (range) | 20 (5–55) | 14 (2–50) | 21 (16–24) | |
| Lesion localization, n (%) | n=16 | n=8 | n=5 | 0.313 |
| Lower extremity | 7 (43.8) | 3 (37.5) | 1 (20.0) | |
| Upper extremity | 3 (18.8) | 1 (12.5) | 0 (0.0) | |
| Trunk | 3 (18.8) | 1 (12.5) | 0 (0.0) | |
| Trunk+lower extremity | 1 (6.3) | 2 (25.0) | 0 (0.0) | |
| Trunk+upper extremity | 1 (6.3) | 0 (0.0) | 1 (20.0) | |
| Head and neck | 1 (6.3) | 1 (12.5) | 3 (60.0) | |
| Cho classification for AVMs*, n (%) | | | | 0.960 |
| I | 1 (7.7) | 0 (0.0) | 0 (0.0) | |
| II | 1 (7.7) | 0 (0.0) | 0 (0.0) | |
| IIIa | 5 (38.5) | 4 (66.7) | 3 (60.0) | |
| IIIb | 6 (46.2) | 2 (33.3) | 2 (40.0) | |
| Schobinger classification for AVMs,† n (%) | n=13 | n=6 | n=5 | 0.037 |
| 1 | 0 (0.0) | 2 (33.3) | 0 (0.0) | |
| 2 | 4 (30.8) | 2 (33.3%) | 4 (80.0) | |
| 3 | 8 (61.5) | 2 (33.3) | 0 (0.0) | |
| 4 | 1 (7.7) | 0 (0.0) | 1 (20.0) | |
| Extremity length discrepancy, n (%) | n=16 | n=8 | n=5 | 1.000 |
| Yes | 4 (25.0) | 2 (25.0) | 1 (20.0) | |
| No | 12 (75.0) | | | |
| Associated segmental overgrowth, n (%) | n=16 | n=8 | n=5 | 0.117 |
| Yes | 11 (68.8) | 2 (25.0) | 2 (40.0) | |
| No | 5 (31.3) | 6 (75) | 3 (60.0) | |
| Progression, n (%) | n=13 | n=6 | n=5 | 0.024 |
| Yes | 10 (76.9) | 1 (16.7) | 1 (20.0) | |
| No | 3 (23.1) | 5 (83.3) | 4 (80.0) | |

AVM indicates arteriovenous malformation; BRAF, V-Raf murine sarcoma viral oncogene homolog B; MAP2K1, mitogen-activated protein kinase kinase 1; PV, pathogenic variant; and RAS, rat sarcoma virus.

*Cho classification according to Cho et al.[16]

†Schobinger classification according to Finn et al.[17]

‡Fisher's exact test for categorial data.

anomalies that may have overlapping clinical features with AVMs (intramuscular fast-flow vascular anomaly; patients 12 and 15), similar to patients described by Goss et al[32] and Sudduth et al.[33]

In general, our results suggest that *RAS* variants are characterized by more advanced disease stage according to Schobinger and higher progression rates (69%), which may pave the way for individualized and intensified multimodal treatment regimens according to the underlying PVs. In a cohort of 18 extracranial AVMs, El Sissy et al[11] also found a higher progression rate of the 6 patients with *KRAS* PVs compared with 7 patients with *MAP2K1* PVs. This finding is therefore now being replicated in a second cohort. Further, we found, that lesions with *KRAS* PVs tend to present a more aggressive infiltrative growth pattern across multiple tissue layers, which has not yet been established

in the literature. However, these preliminary findings should be interpreted with caution due to the small sample sizes. If confirmed in further studies, this may also have an impact on patient stratification and may further shift the choice of therapy options.

*BRAF* PVs have previously been detected in tissue samples from various intra- and extracranial vascular anomalies including fast-flow malformations, isolated slow-flow malformations, and vascular tumors such as pyogenic granulomas.[8,11,34,35] In these cohorts, all reported cases presented the *BRAF* PV, c.1799T>A, p.Val-600Glu, which was also the predominating *BRAF* PV in our study. Additionally, in 1 case (patient 17), we identified a novel mosaic *BRAF* variant, c.1517+2_1517+3insTACT-CAGGT, that predicts the insertion of 3 amino acids in the protein p.Arg506_Lys507insLeuLeuArg. Comparing the clinical phenotype associated with the few cases

**Table 4.** Comparison of Tissue Involvement Among the KRAS, HRAS, NRAS, BRAF, and MAP2K1 PV Carriers

| Clinical characteristics | KRAS | HRAS | NRAS | BRAF | MAP2K1 | P value[†] |
|---|---|---|---|---|---|---|
| Age, y | n=10 | n=5 | n=1 | n=8 | n=5 | |
| Median (range) | 24 (5–55) | 17 (14–20) | | 14 (2–50) | 21 (16–24) | |
| Lesion tissue involvement*, n (%) | n=10 | n=5 | n=1 | n=8 | n=5 | 0.036 |
| (Sub)cutaneous | 1 (10.0) | 0 (0.0) | 1 (100.0) | 3 (37.5) | 3 (60.0) | |
| Intramuscular | 1 (10.0) | 3 (60.0) | 0 (0.0) | 3 (37.5) | 0 (0.0) | |
| Multiple layers[†] | 8 (80.0) | 2 (40.0) | 0 (0.0) | 2 (25.0) | 2 (40.0) | |

BRAF, V-Raf murine sarcoma viral oncogene homolog B; HRAS, Harvey rat sarcoma viral oncogene homolog; MAP2K1, mitogen-activated protein kinase kinase 1; NRAS, neuroblastoma RAS viral oncogene homolog; and PV, pathogenic variant.

*Multiple tissue layers include (sub)cutaneous, muscular, and osseous involvement of the vascular anomaly.

†Fisher's exact test for categorial data.

where *BRAF* PVs have been previously described in the literature,[8,11,34,35] 8 patients with *BRAF* PVs in our cohort showed similarly variable clinical phenotypes including AVMs of limited extension (patients 17, 18, 22, and 23), a more extensive AVM with multiple-layer tissue involvement (patient 20), a complex combined Parkes–Weber-like phenotype (patient 21), a subungual VM (patient 24), and a diffuse infantile fibromatosis (patient 19). Associated segmental overgrowth and multiple tissue layer involvement were observed in 25% each. The latter was less prevalent compared with *KRAS* PVs, which may indicate better and less challenging conditions for surgical or interventional treatment approaches. While the nature of vascular anomalies varied, patients had less severe symptoms and a lower progression rate compared with those with *RAS* PVs.

*MAP2K1* PVs were found in 5 cases (17%) of our cohort with the recurrent *MAP2K1* PV, c.171G>T, p.Lys57Asn, found twice, while 3 other *MAP2K1* PVs were identified in single cases. These PVs were all missense or small in-frame deletions affecting amino acid residues adjacent to or within the protein's negative regulatory domain and have been previously reported in an AVM cohort by Couto et al.[12] Several of these variants have been found in cancers and shown to increase MAP2K1 activity.[36,37] In our cohort, patients with *MAP2K1* PVs all had AVMs, which is in contrast to the *RAS* and *BRAF* PVs including a broader clinical spectrum of vascular anomalies. A certain selection bias for this observation cannot be excluded, and this observation needs yet to be evaluated in other cohorts. Lesions with *MAP2K1* PVs were classified as Schobinger stage II in 80% and were accompanied by segmental or local overgrowth in 20%. Similar to the *BRAV* PVs in our cohort, *MAP2K1* PVs presented lower progression rates (20%) compared with *KRAS* PVs. El Sissy et al[11] reported comparable results regarding differences in Schobinger classification and progression rates after treatment (29% versus 100%) among 7 patients with *MAP2K1* and 6 patients with *KRAS* PVs in facial AVMs. At this preliminary state of knowledge, these results should be interpreted with the limitation

that small group sizes were analyzed in our cohort as well as the cohorts reported previously.

*RAS*, *BRAF*, or *MAP2K1* have long been implicated in various malignancies, in which they play a driving role in tumor growth. This knowledge has led to the development of targeted therapies using small molecule inhibitors of the RAS/MAPK pathway, which are also considered as potential new therapies for vascular anomalies driven by overactivation of this pathway. Mitogen-activated protein kinase kinase inhibition with trametinib was used off-label in 2 patients in this cohort; both patients subsequently showed a reduction of symptoms and no progression. Lekwuttikarn et al[38] reported an 11-year-old female patient presenting with an extracranial *MAP2K1*-mutated AVM treated by trametinib. One month after treatment initiation, the vascular malformation presented with clinically decreased perfusion and discoloration, and magnetic resonance imaging after 6 months confirmed an objective decrease in size. Al-Olabi et al[8] reported the treatment of AVM-*BRAF* mutant zebrafish with the *BRAF* inhibitor (vemurafinib), which resulted in hemodynamic improvement through less distorted vasculature. One patient in our cohort (patient 20) with an AVM of the foot due to a *BRAF* mutation was treated with the *BRAF* inhibitor dabrafenib due to pain and lack of promising surgical or interventional treatment approaches. Under this therapy, the pain quickly abated, and she had a substantial functional improvement, while no severe adverse events occurred during this therapy. A specific *KRAS* G12C inhibitor (sotorasib) was recently developed for the treatment of *KRAS* G12C–mutated non-small-cell lung cancer.[39] The latter may be suggested specifically for patients with AVM with the *KRAS* G12C PVs that made up an important part of all *KRAS* PVs in our cohort. Sotorasib would represent an even more specific targeted treatment compared with unselective mitogen-activated protein kinase kinase inhibition, for example, with trametinib. This approach may harbor potential benefits, especially in light of the high progression rates in patients with *KRAS* AVMs but will need further study in clinical trials.

Generally, the growing body of literature as well as this study support the notion that the clinical spectrum of vascular anomalies driven by PVs in components of the canonical RAS/MAPK pathway is becoming broader than anticipated after the first published findings in selected patient cohorts, and together with their broadening the clinical spectra associated with individual genes also tend to merge. There is still a predominance of fast-flow anomalies, but mixed and low-flow malformations such as VMs also occur. Notably, *MAP2K1* variants have exclusively been observed in AVMs so far. The validation and further resolution of genotype–phenotype correlations in vascular anomalies deserve continued efforts and studies in larger cohorts, before they become a routine basis of clinical decision making. As such, this works in a hypothesis-generating manner to set up larger multicenter cohorts, potentially on the basis of registries, as large randomized controlled trials on vascular anomalies are unlikely to being realized in the near future.[40]

This study reveals preliminary associations of *RAS/BRAF/MAP2K1* mosaicism with clinical phenotypes of extracranial vascular anomalies. Lesions with *KRAS* PVs tended to show more infiltrative growth patterns across multiple tissue layers. Furthermore, *RAS* variants were characterized by more advanced disease stages and potentially higher progression rates, reflecting a more aggressive phenotype. The benefit of combining clinical and genetic diagnostics may promote more individualized treatment regimens according to the underlying PV such as by adding targeted therapeutics to multidisciplinary care.

## ARTICLE INFORMATION

### Affiliations

Department of Radiology (V.F.S., M.S., A.S., J.R., M.A.K., M.W.) and Interdisziplinäres Zentrum für Gefäßanomalien (IZGA) (V.F.S., M.S., A.S., B.H., J.H., A.W., J.R., M.A.K., M.W.), LMU University Hospital, LMU Munich, München, Germany; Division of Pediatric Hematology and Oncology, Department of Pediatric and Adolescent Medicine, University Medical Center Freiburg, University of Freiburg, Germany (F.G.K., J.C., A.H.); Clinic and Policlinic of Radiology, Martin-Luther University Halle-Wittenberg, Halle (Saale), Germany (C.G., L.H., B.C., R.B., W.A.W.); Department of Otorhinolaryngology, Regensburg University Medical Center, Regensburg, Germany (V.V., C.T.S.); Department of Pediatric and Adolescent Surgery, Paracelsus Medical University Hospital, Salzburg, Austria (A.-J.M.); Department of Diagnostic and Interventional Radiology (W.U.) and Department of Plastic and Hand Surgery (J.B.W.), University of Freiburg Medical Centre, Medical Faculty of the University of Freiburg, Freiburg, Germany; Department of Pediatric Surgery, Dr. von Hauner Children's Hospital, LMU University Hospital, LMU Munich, München, Germany (B.H., J.H., A.W.); and Institute of Human Genetics, University Hospital Magdeburg, Magdeburg, Germany (D.S., M.Z.).

### Acknowledgments

### Sources of Funding

### Disclosures

### Supplemental Material

Table S1

## REFERENCES

1. Wassef M, Borsik M, Cerceau P, Faucon B, Laurian C, Le Clerc N, Lemarchand-Venencie F, Massoni C, Salvan D, Bisdorff-Bresson A. Classification des tumeurs et malformations vasculaires. Apport de la classification ISSVA 2014/2018. Article in French. *Ann Pathol*. 2021;41:58–70. doi: 10.1016/j.annpat.2020.11.004

2. Schmidt VF, Olivieri M, Häberle B, Masthoff M, Deniz S, Sporns PB, Wohlgemuth WA, Wildgruber M. Interventional treatment options in children with extracranial vascular malformations. *Hamostaseologie*. 2022;42:131–141. doi: 10.1055/a-1728-5686

3. Schmidt VF, Masthoff M, Goldann C, Deniz S, Öcal O, Häberle B, Köhler M, Seidensticker M, Ricke J, Wohlgemuth WA, et al. Percutaneous sclerotherapy of venous malformations of the hand: a multicenter analysis. *Cardiovasc Intervent Radiol*. 2021;44:1543–1550. doi: 10.1007/s00270-021-02926-x

4. Schmidt VF, Masthoff M, Goldann C, Ehrl D, Deniz S, Öcal O, Seidensticker M, Ricke J, Köhler M, Brill R, et al. Image-guided embolization of arteriovenous malformations of the hand using ethylene-vinyl alcohol copolymer. *Diagn Interv Radiol*. 2022;28:486–494. doi: 10.5152/dir.2022.21644

5. Schmidt VF, Masthoff M, Czihal M, Cucuruz B, Häberle B, Brill R, Wohlgemuth WA, Wildgruber M. Imaging of peripheral vascular malformations—current concepts and future perspectives. *Mol Cell Pediatr*. 2021;8:19. doi: 10.1186/s40348-021-00132-w

6. Queisser A, Seront E, Boon LM, Vikkula M. Genetic basis and therapies for vascular anomalies. *Circ Res*. 2021;129:155–173. doi: 10.1161/CIRCRESAHA.121.318145

7. Nathan N, Keppler-Noreuil KM, Biesecker LG, Moss J, Darling TN. Mosaic disorders of the PI3K/PTEN/AKT/TSC/MTORC1 signaling pathway. *Dermatol Clin*. 2017;35:51–60. doi: 10.1016/j.det.2016.07.001

8. Al-Olabi L, Polubothu S, Dowsett K, Andrews KA, Stadnik P, Joseph AP, Knox R, Pittman A, Clark G, Baird W, et al. Mosaic RAS/MAPK variants cause sporadic vascular malformations which respond to targeted therapy. *J Clin Invest*. 2018;128:1496–1508. doi: 10.1172/JCI98589

9. Nikolaev SI, Vetiska S, Bonilla X, Boudreau E, Jauhiainen S, Rezai Jahromi B, Khyzha N, DiStefano PV, Suutarinen S, Kiehl TR, et al. Somatic activating KRAS mutations in arteriovenous malformations of the brain. *N Engl J Med*. 2018;378:250–261. doi: 10.1056/NEJMoa1709449

10. Schmidt VF, Wieland I, Wohlgemuth WA, Ricke J, Wildgruber M, Zenker M. Mosaic rasopathy due to KRAS variant G12D with segmental overgrowth and associated peripheral vascular malformations. *Am J Med Genet A*. 2021;185:3122–3128. doi: 10.1002/ajmg.a.62386

11. El Sissy FN, Wassef M, Faucon B, Salvan D, Nadaud S, Coulet F, Adle-Biassette H, Soubrier F, Bisdorff A, Eyries M. Somatic mutational landscape of extracranial arteriovenous malformations and phenotypic correlations. *J Eur Acad Dermatol Venereol*. 2022;36:905–912. doi: 10.1111/jdv.18046

12. Couto JA, Huang AY, Konczyk DJ, Goss JA, Fishman SJ, Mulliken JB, Warman ML, Greene AK. Somatic MAP2K1 mutations are

associated with extracranial arteriovenous malformation. *Am J Hum Genet*. 2017;100:546–554. doi: 10.1016/j.ajhg.2017.01.018

13. Ten Broek RW, Eijkelenboom A, van der Vleuten CJM, Kamping EJ, Kets M, Verhoeven BH, Grünberg K, Schultze Kool LJ, Tops BBJ, Ligtenberg MJL, et al. Comprehensive molecular and clinicopathological analysis of vascular malformations: a study of 319 cases. *Genes Chromosomes Cancer*. 2019;58:541–550. doi: 10.1002/gcc.22739

14. Wei T, Shalin S, Draper E, Miller E, Zhang H, Sun R, Lee M, Albert G, Richter GT. Abnormal elastin and collagen deposition is present in extracranial arteriovenous malformations: a comparison to intracranial disease. *Histol Histopathol*. 2019;34:1355–1363. doi: 10.14670/HH-18-129

15. Greene AK, Liu AS, Mulliken JB, Chalache K, Fishman SJ. Vascular anomalies in 5,621 patients: guidelines for referral. *J Pediatr Surg*. 2011;46:1784–1789. doi: 10.1016/j.jpedsurg.2011.05.006

16. Cho SK, Do YS, Shin SW, Kim DI, Kim YW, Park KB, Kim EJ, Ahn HJ, Choo SW, Choo IW. Arteriovenous malformations of the body and extremities: analysis of therapeutic outcomes and approaches according to a modified angiographic classification. *J Endovasc Ther*. 2006;13:527–538. doi: 10.1583/05-1769.1

17. Finn MC, Glowacki J, Mulliken JB. Congenital vascular lesions: clinical application of a new classification. *J Pediatr Surg*. 1983;18:894–900. doi: 10.1016/S0022-3468(83)80043-8

18. Puig S, Aref H, Chigot V, Bonin B, Brunelle F. Classification of venous malformations in children and implications for sclerotherapy. *Pediatr Radiol*. 2003;33:99–103. doi: 10.1007/s00247-002-0838-9

19. Little J, Higgins JP, Ioannidis JP, Moher D, Gagnon F, von Elm E, Khoury MJ, Cohen B, Davey-Smith G, Grimshaw J, et al. STrengthening the REporting of Genetic Association studies (STREGA)—an extension of the STROBE statement. *Genet Epidemiol*. 2009;33:581–598. doi: 10.1002/gepi.20410

20. *ISSVA classification of vascular anomalies ©2018 International Society for the Study of Vascular Anomalies*. Published April 2014. Date updated May 2018. Assessed May 25, 2023. issva.org/classification; https://www.issva.org/UserFiles/file/ISSVA-Classification-2018.pdf

21. Oka M, Kushamae M, Aoki T, Yamaguchi T, Kitazato K, Abekura Y, Kawamata T, Mizutani T, Miyamoto S, Takagi Y. KRAS G12D or G12V mutation in human brain arteriovenous malformations. *World Neurosurg*. 2019;126:e1365–e1373. doi: 10.1016/j.wneu.2019.03.105

22. Goss JA, Huang AY, Smith E, Konczyk DJ, Smits PJ, Sudduth CL, Stapleton C, Patel A, Alexandrescu S, Warman ML, et al. Somatic mutations in intracranial arteriovenous malformations. *PLoS One*. 2019;14:e0226852. doi: 10.1371/journal.pone.0226852

23. Nozawa A, Ozeki M, Niihori T, Suzui N, Miyazaki T, Aoki Y. A somatic activating KRAS variant identified in an affected lesion of a patient with gorham-stout disease. *J Hum Genet*. 2020;65:995–1001. doi: 10.1038/s10038-020-0794-y

24. Eijkelenboom A, van Schaik FMA, van Es RM, Ten Broek RW, Rinne T, van der Vleuten C, Flucke U, Ligtenberg MJL, Rehmann H. Functional characterisation of a novel class of in-frame insertion variants of KRAS and HRAS. *Sci Rep*. 2019;9:8239. doi: 10.1038/s41598-019-44584-7

25. Konczyk DJ, Goss JA, Smits PJ, Huang AY, Al-Ibraheemi A, Sudduth CL, Warman ML, Greene AK. Arteriovenous malformation associated with a HRAS mutation. *Hum Genet*. 2019;138:1419–1421. doi: 10.1007/s00439-019-02072-y

26. Siegel DH, Cottrell CE, Streicher JL, Schilter KF, Basel DG, Baselga E, Burrows PE, Ciliberto HM, Vigh-Conrad KA, Eichenfield LF, et al. Analyzing the genetic spectrum of vascular anomalies with overgrowth via cancer genomics. *J Invest Dermatol*. 2018;138:957–967. doi: 10.1016/j.jid.2017.10.033

27. Ozeki M, Aoki Y, Nozawa A, Yasue S, Endo S, Hori Y, Matsuoka K, Niihori T, Funayama R, Shirota M, et al. Detection of NRAS mutation in cell-free DNA biological fluids from patients with kaposiform lymphangiomatosis. *Orphanet J Rare Dis*. 2019;14:215. doi: 10.1186/s13023-019-1191-5

28. Barclay SF, Inman KW, Luks VL, McIntyre JB, Al-Ibraheemi A, Church AJ, Perez-Atayde AR, Mangray S, Jeng M, Kreimer SR, et al. A somatic activating NRAS variant associated with kaposiform lymphangiomatosis. *Genet Med*. 2019;21:1517–1524. doi: 10.1038/s41436-018-0390-0

29. Manevitz-Mendelson E, Leichner GS, Barel O, Davidi-Avrahami I, Ziv-Strasser L, Eyal E, Pessach I, Rimon U, Barzilai A, Hirshberg A, et al. Somatic NRAS mutation in patient with generalized lymphatic anomaly. *Angiogenesis*. 2018;21:287–298. doi: 10.1007/s10456-018-9595-8

30. Chowers G, Abebe-Campino G, Golan H, Vivante A, Greenberger S, Soudack M, Barkai G, Fox-Fisher I, Li D, March M, et al. Treatment of severe kaposiform lymphangiomatosis positive for NRAS mutation by MEK inhibition. *Pediatr Res*. 2023;94:1911–1915. doi: 10.1038/s41390-022-01986-0

31. Groesser L, Peterhof E, Evert M, Landthaler M, Berneburg M, Hafner C. BRAF and RAS mutations in sporadic and secondary pyogenic granuloma. *J Invest Dermatol*. 2016;136:481–486. doi: 10.1038/JID.2015.376

32. Goss JA, Konczyk DJ, Smits PJ, Kozakewich HPW, Alomari AI, Al-Ibraheemi A, Taghinia AH, Dickie BH, Adams DM, Fishman SJ, et al. Intramuscular fast-flow vascular anomaly contains somatic MAP2K1 and KRAS mutations. *Angiogenesis*. 2019;22:547–552. doi: 10.1007/s10456-019-09678-w

33. Sudduth CL, McGuire AM, Smits PJ, Konczyk DJ, Al-Ibraheemi A, Fishman SJ, Greene AK. Arteriovenous malformation phenotype resembling congenital hemangioma contains KRAS mutations. *Clin Genet*. 2020;98:595–597. doi: 10.1111/cge.13833

34. Zenner K, Jensen DM, Dmyterko V, Shivaram GM, Myers CT, Paschal CR, Rudzinski ER, Pham MM, Cheng VC, Manning SC, et al. Somatic activating BRAF variants cause isolated lymphatic malformations. *HGG Adv*. 2022;3:100101. doi: 10.1016/j.xhgg.2022.100101

35. Strobel K, Maurus K, Hamm H, Roth S, Goebeler M, Rosenwald A, Wobser M. Recurrent alterations in the MAPK pathway in sporadic pyogenic granuloma of childhood. *Acta Derm Venereol*. 2022;102:adv00715. doi: 10.2340/actadv.v102.1119

36. Nikolaev SI, Rimoldi D, Iseli C, Valsesia A, Robyr D, Gehrig C, Harshman K, Guipponi M, Bukach O, Zoete V, et al. Exome sequencing identifies recurrent somatic MAP2K1 and MAP2K2 mutations in melanoma. *Nat Genet*. 2012;44:133–139. doi: 10.1038/ng.1026

37. Choi YL, Soda M, Ueno T, Hamada T, Haruta H, Yamato A, Fukumura K, Ando M, Kawazu M, Yamashita Y, et al. Oncogenic MAP2K1 mutations in human epithelial tumors. *Carcinogenesis*. 2012;33:956–961. doi: 10.1093/carcin/bgs099

38. Lekwuttikarn R, Lim YH, Admani S, Choate KA, Teng JMC. Genotype-guided medical treatment of an arteriovenous malformation in a child. *JAMA Dermatol*. 2019;155:256–257. doi: 10.1001/jamadermatol.2018.4653

39. Skoulidis F, Li BT, Dy GK, Price TJ, Falchook GS, Wolf J, Italiano A, Schuler M, Borghaei H, Barlesi F, et al. Sotorasib for lung cancers with KRAS p.G12C mutation. *N Engl J Med*. 2021;384:2371–2381. doi: 10.1056/NEJMoa2103695

40. Schmidt VF, Masthoff M, Vielsmeier V, Seebauer CT, Cangir Ö, Meyer L, Mükke A, Lang W, Schmid A, Sporns PB, et al. Clinical outcome and quality of life of multimodal treatment of extracranial arteriovenous malformations: the apollon study protocol. *Cardiovasc Intervent Radiol*. 2023;46:142–151. doi: 10.1007/s00270-022-03296-8